

## Two-dimensional adatom gas on the Si(111)-( $\sqrt{3} \times \sqrt{3}$ )-Ag surface detected through changes in electrical conduction

Yuji Nakajima, Gen Uchida, Tadaaki Nagao, and Shuji Hasegawa

*Department of Physics, School of Science, University of Tokyo, Hongo, Bunkyo-ku, Tokyo 113, Japan*

(Received 19 July 1996)

When Ag adatoms were deposited on top of the Si(111)- $\sqrt{3} \times \sqrt{3}$ -Ag surface at room temperature with less than a critical coverage  $\Theta_C$  ( $\sim 0.03$  atomic layer), they were found to exist as a supersaturated metastable two-dimensional gas phase, which made the surface electrical conductance extremely high. With the coverage beyond  $\Theta_C$ , the gas phase began to nucleate into three-dimensional microcrystals, leading to a steep reduction in the electrical conductance. A kinetic overshoot beyond the critical supersaturation for nucleation was also detected in *in situ* conductance measurements during the Ag deposition. [S0163-1829(96)03343-7]

Two-dimensional adatom gas (2DAG) on a solid surface is an intermediate state between the vapor and solid phases, which plays an important role in various dynamical phenomena occurring on the surface. During thermal desorption processes, for example, atoms constituting the crystal surface or microcrystals leave their sites, and migrate for a while making a 2DAG before evaporating into vacuum. The 2DAG is nearly equilibrated with the ‘‘reservoirs’’ (2D or 3D islands) through reversible attachment and detachment of atoms between them.<sup>1</sup> This process modifies the order of reaction. In crystal growths, conversely, atoms deposited onto a surface are highly mobile for a while before being incorporated into the crystal structure. The surface diffusion length in the 2DAG in this case determines the style of the atomic-layer growth (step-flow type or 2D/3D islands nucleation type). The nucleation of the 2DAG, especially, has another interesting aspect; it is an evolution from a nonequilibrium state, in which adatoms are supersaturated, to an equilibrium thermodynamic state. In this way, the observed results (the desorption rates, surface morphologies, islands density, and so on) have been consistently understood by assuming mobile atoms in the 2DAG, although the gas is not directly detected.

We report here that the 2DAG of Ag deposited on top of the Si(111)- $\sqrt{3} \times \sqrt{3}$ -Ag surface ( $\sqrt{3}$ -surface in short) at room temperature (RT) was directly detected in *in situ* measurements of surface electrical conductance. The 2DAG was found to remarkably enhance the electrical conduction. With less than a critical coverage  $\Theta_C \sim 0.03$  monolayer (ML) of the Ag adatoms, no stable nuclei were created to retain the supersaturated metastable 2DAG existing on the surface, keeping the conductance high. With the coverage beyond  $\Theta_C$ , stable 3D nuclei began to be formed by capturing the adatoms in the 2DAG to return to a lower equilibrium adatom density, resulting in a steep reduction in electrical conductance. A kinetic overshoot beyond the critical supersaturation for the nucleation was also detected in the conductance measurements during the Ag deposition. The surface conductance measurements have thus turned out to be a truly *in situ* and real-time monitoring method for dynamical atomistic processes occurring on the surface. A possible mechanism for the conductance enhancement by the 2DAG on top of the surface will be discussed in connection with the surface-state conductivity and the band bending.

The  $\sqrt{3}$  surface is now fully understood on the atomic and electronic structures.<sup>2</sup> The Ag atoms make covalent bonds with the substrate Si atoms, leaving no dangling bonds. This results in the extreme reductions in the surface energy as well as in the corrugation of the surface topography, compared with the Si(111)- $7 \times 7$  clean surface. Therefore, when additional Ag atoms are deposited onto this surface at RT, the Ag adatoms migrate with extremely high mobility to nucleate into 3D microcrystals, leaving the  $\sqrt{3}$  surface scarcely covered. These microcrystals are observed by reflection-high-energy electron diffraction (RHEED) and scanning electron microscopy (SEM) as shown in Fig. 1. The 3D microcrystals tend to nucleate in the vicinity of other microcrystals to make its colonies [Figs. 1(b) and 1(c)]. When the coverage of Ag is increased, additional nuclei are formed [Fig. 1(d)], so that the nucleation is heterogeneous.

The same experimental method as in previous reports<sup>3</sup> was adopted. The measurements were performed in an ultra-high vacuum chamber with a RHEED system, a sample holder for four-probe conductivity measurements, and an alumina-coated W basket as a Ag evaporator. An *n*-type Si(111) wafer of 100  $\Omega$  cm resistivity and  $30 \times 4 \times 0.5$  mm<sup>2</sup> in size was used. The surface was cleaned to obtain a clear  $7 \times 7$  RHEED pattern, by several flash heatings up to 1500 K for 10 s with a direct current of 9 A through it. The  $\sqrt{3}$  surface was prepared by 1 ML Ag deposition with a constant rate of 0.17 ML/min onto the  $7 \times 7$  substrate at 760 K, and then the sample was cooled down. The electrical resistance of the central portion of the wafer, under isothermal conditions at RT, was measured as a voltage drop between a pair of Ta wire contacts, with a constant current of 10  $\mu$ A supplied through the Ta end-clamp electrodes. The RHEED beam was always turned off during the electrical measurements. To measure the influence of radiation from the Ag evaporator on the conductivity, the same type of empty evaporator was placed near the Ag evaporator. Even if the empty evaporator was heated up to the evaporating temperature, its radiation was too weak to change the resistance, as in Ref. 3.

Figure 2 shows the changes in resistance during and after the Ag deposition at RT. The resistances are normalized by the initial values  $R_0$ . The amounts of the deposited Ag,

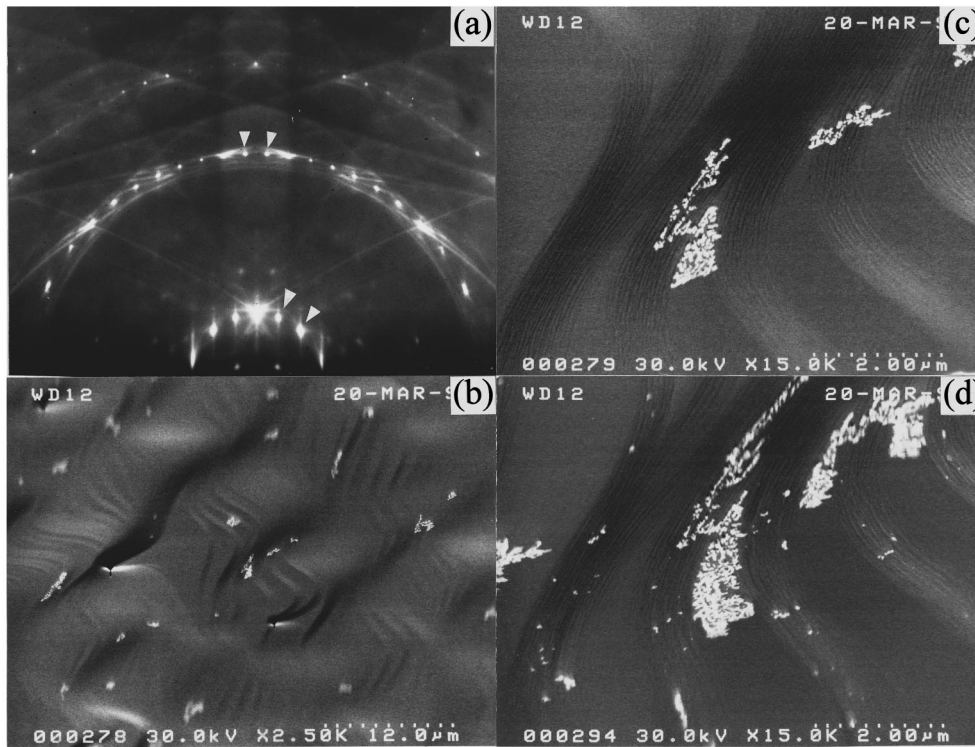


FIG. 1. (a) RHEED pattern after 4.5-ML-Ag deposition onto the  $\sqrt{3} \times \sqrt{3}$ -Ag surface at RT. The  $\sqrt{3} \times \sqrt{3}$  superspots indicated by arrow heads remain strong even after the transmission-type diffraction spots from the Ag 3D microcrystals appear. (b) A grazing-incidence UHV-SEM image after about 0.2-ML-Ag deposition onto the  $\sqrt{3} \times \sqrt{3}$ -Ag surface at RT, and (c) its magnified image showing the atomic steps and colonies of Ag 3D microcrystals. (d) With further deposition up to around 0.4 ML, new additional microcrystals appear.

$\Theta_{Ag}$ , are decreased from curve (a) to (i). For curves (a)–(e), the same features as in previous reports<sup>3</sup> are seen; the resistance remarkably drops by several tens percent with Ag deposition of only around 0.03 ML, and after making a small overshoot, it continues to decrease moderately with further deposition. After the deposition is stopped, the resistance steeply rises. By carefully looking at the rises in resistance after the deposition stops, however, a slight difference is noticed; in curves (a) and (b), the resistance rises monotonically, while in curves (c)–(e), a shoulder is seen during the steep rise. In contrast, for curves (g)–(i), where the deposition is stopped before reaching the coverage corresponding to the overshoot, the resistance change is quite different; it remains almost constant after the deposition is stopped. So the phenomena occurring on the surface are completely different between curves (a)–(e) and (g)–(i), of which  $\Theta_{Ag}$  are more and less of the critical coverage  $\Theta_C$  ( $\sim 0.03$  ML) corresponding to the overshoot in resistance drop, respectively.

Figure 3 shows the changes in resistance during a series of six intermittent depositions. Small constant amount of Ag is deposited during each deposition interval, which causes an abrupt drop in resistance. While during the interruption intervals (a) and (b) the resistance remains constant, it increases a little during (c). During the interruption intervals (d)–(f), it increases steeply.

The upper panel of Fig. 4 shows the changes in resistance during the sequence of two successive depositions. During the first depositions and the following interruption intervals for all curves, the resistance changes in the same way as (d) in Fig. 2. Immediately after the start of the second deposi-

tions, the resistance drops abruptly again. In curves (d) and (e), the resistance decreases slowly after this drop without making an overshoot. By stopping the deposition, the resistance steeply rises with making a shoulder like (c) and (d) in Fig. 2. When, as shown in curves (a) and (b) in Fig. 4, the second depositions are stopped before reaching the bending point in curves (d) and (e), the resistance recovers monotonically, but not in a simple exponential way.

The lower panel of Fig. 4 shows similar measurements during the sequence of two successive depositions, where the amounts of the first depositions are changed in the range over  $\Theta_C$ , and a constant amount of Ag is deposited at the second stage. When the first-deposition coverage is small like curve (f), the resistance drops quickly by starting the second deposition. On the other hand, when the first deposition is prolonged like curve (i), the resistance drops slowly at the second-deposition stage.

The above results can be understood by taking into account the atomistic processes which are observed in the SEM and RHEED in Fig. 1. Curve (a) in Fig. 2 was tentatively explained through the following mechanism in previous papers.<sup>3</sup> The deposited Ag adatoms which are individually mobile before being captured by 3D nuclei give rise to the abrupt decrease in resistance at the beginning of the deposition. The recovering rise in resistance by the stopping of the deposition corresponds to the aggregation of these individual adatoms in the 2DAG into 3D nuclei. This speculation was confirmed by Natori *et al.*<sup>4</sup> using Monte Carlo simulation of the time evolution of the number density of the adatoms. They have shown that the adatom density changes in close

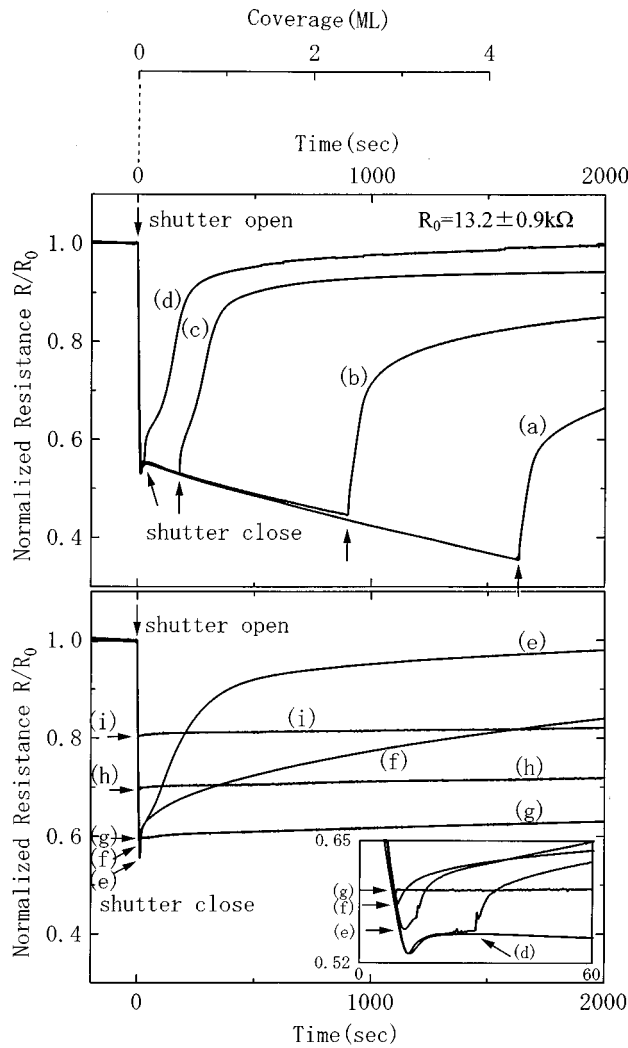


FIG. 2. The resistance changes during and after the Ag deposition (rate: 0.16 ML/min) onto the Si(111)- $\sqrt{3} \times \sqrt{3}$ -Ag surface at RT. The deposition coverages  $\Theta_{\text{Ag}}$  are (a) 4.5 ML, (b) 2.1 ML, (c) 0.52 ML, (d) 0.081 ML, (e) 0.042 ML, (f) 0.029 ML, (g) 0.025 ML, (h) 0.015 ML, and (i) 0.0079 ML, respectively. The inset shows the points when the depositions are stopped for the curves (d)–(g).

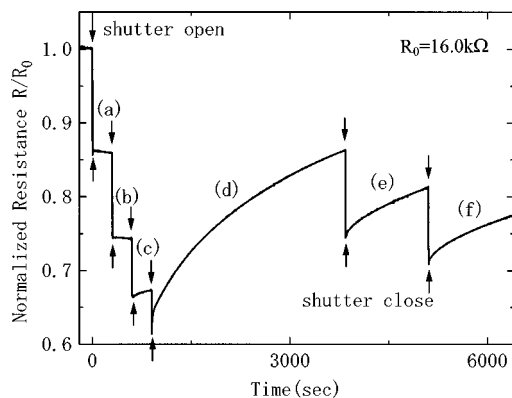


FIG. 3. The resistance change during intermittent Ag depositions. Small constant amount of Ag,  $\Delta\Theta_{\text{Ag}}$ , is deposited during the intervals of 2 sec indicated by the arrows. The deposition rate is 0.24 ML/min, so that  $\Delta\Theta_{\text{Ag}} \sim 0.008$  ML. (a)–(f) denote the interrupted intervals.

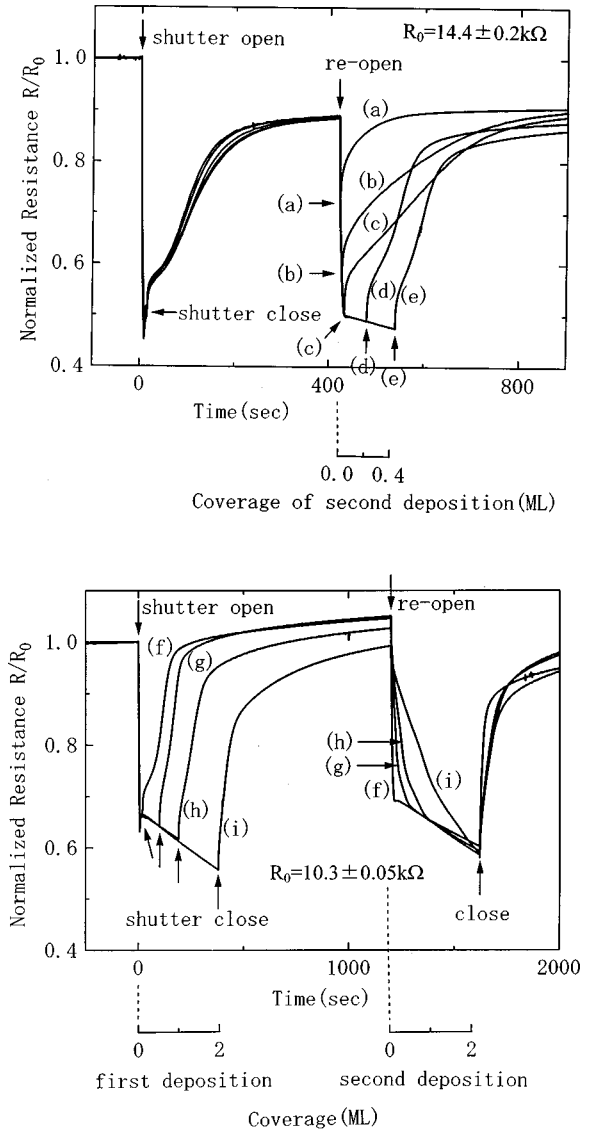


FIG. 4. The resistance changes during the sequence of two successive Ag depositions. Upper panel: The first-deposition coverages are the same 0.056 ML for all curves. The second-deposition coverages are (a) 0.0074 ML, (b) 0.026 ML, (c) 0.048 ML, (d) 0.22 ML, and (e) 0.44 ML, respectively, with the rate of 0.22 ML/min. Lower panel: The first-deposition coverages are (f) 0.1 ML, (g) 0.5 ML, (h) 1 ML, and (i) 2 ML, respectively, with the rate of 0.31 ML/min, while the second-deposition coverages are the same 2.2 ML for all curves.

resemblance with the resistance curves (a) and (b) in Fig. 2; the adatom density steeply increases at the beginning of the deposition and makes an overshoot peak, and then it decreases down to a smaller equilibrium density which is determined by balance between the deposition rate and the capturing rate into 3D nuclei. When the deposition is stopped, the adatom density steeply decreases down to a lower equilibrium value where the reversible attachment and detachment of adatom are balanced between the 3D microcrystals and the 2DAG. We have expected that when the deposition is stopped before the coverage reaches the  $\Theta_C$ , no stable nuclei are created to retain the 2DAG. This is the

reason why the resistance remains a small constant even after the deposition stops in our experiment [Figs. 2(g)–2(i)], which is also reproduced by a simulation.<sup>5</sup> When the coverage exceeds the  $\Theta_C$ , the nucleation of adatoms starts. So by stopping the deposition beyond  $\Theta_C$ , the resistance recovers, because the 3D nuclei act as sinks of the 2DAG to decrease the adatom density. Therefore, it is found that the  $\Theta_C$  is the critical coverage for nucleation (limit of metastability of the 2DAG), and corresponds to the critical supersaturation. The resistance curves [Fig. 2(a)–2(d)] make an overshoot just beyond  $\Theta_C$ , which corresponds to a kinetic overshoot beyond the critical supersaturation. When the deposition is stopped at the very vicinity of  $\Theta_C$ , the rise in resistance is much slower as shown in Fig. 2(f) compared with 2(e), where the 2DAG is more supersaturated. So 2(f) is near the condition of the critical slowing down of the nucleation.

In the series of the intermittent depositions (Fig. 3) for  $\Theta_{Ag} < \Theta_C$  [(a)–(c)], the resistance decreases as the adatom density increases, which also indicates that the system is a supersaturated metastable 2DAG. The changes in resistance for  $\Theta_{Ag} > \Theta_C$  [(d)–(f)] correspond to the capture of the adatoms in 2DAG by the existing stable nuclei. The slight increase in resistance during the interruption interval (c) corresponds to the critical slowing down of nucleation.

At the stage of the first depositions in Fig. 4, there is an overshoot in resistance just beyond  $\Theta_C$  because of a kinetic overshoot of supersaturation above the critical supersaturation. On the other hand, at the stage of the second depositions, there are already stable nuclei formed by the first depositions, so the nuclei always capture the impinging adatoms. Thus the supersaturation does not become large enough to make an overshoot. This is reproduced by the simulation.<sup>4</sup> Therefore, the bending point in Figs. 4(d) and 4(e) just after the steep drop at the second deposition stage corresponds to a point when the supersaturation of the adatoms reaches the critical supersaturation and additional stable nuclei begin to nucleate after that.

The curves of Figs. 2(c)–2(e), where the depositions are stopped just beyond  $\Theta_C$ , exhibit a shoulder during the steep rise in resistance after the deposition stops. Figure 4 gives an additional insight into this phenomenon. When the second deposition is stopped before the supersaturation reaches the critical supersaturation [(a) and (b) in Fig. 4], the resistance recovers monotonically because Ag adatoms are just captured by the 3D nuclei already formed in the first deposition. On the other hand, when the second deposition is stopped after the supersaturation reaches the critical supersaturation [(d) and (e) in Fig. 4], the rise in resistance after the deposition stops exhibits a shoulder. So it can be said that the shoulder is an effect of the nucleation of new additional stable nuclei.

The change in the adatom density  $\Theta_{ad}$  in 2DAG can be formally described by the rate equation  $d\Theta_{ad}/dt = R - \Theta_{ad}/\tau$ , where  $R$  denotes the deposition rate, and  $\tau$  represents a ‘‘lifetime’’ of the adatoms in 2DAG against being captured by 3D nuclei. So  $\tau$  depends on the number density of the sinks (stable nuclei). On the virgin surface, there is no 3D nuclei to be  $\tau = \infty$ . Thus  $\Theta_{ad} = Rt$  up to  $\Theta_C$ . This corresponds to the steep drop in resistance at the beginning of the first deposition in the lower panel in Fig. 4 (as well as in Fig. 2), and also nearly corresponds to the

change at the beginning of the second deposition of (f) where stable 3D nuclei are very rare. However, when the deposited amount in the first deposition is increased like curves (g)–(i) in Fig. 4, becomes smaller at the second-deposition stage, because of the larger density of the stable nuclei already existing. At the beginning of the second deposition,  $\tau$  should be constant, but different for the respective curves, so that  $\Theta_{ad}$  is solved as  $\Theta_{ad} = R\tau(1 - e^{-t/\tau})$  until the additional new stable nuclei begin to appear. This qualitatively describes the trend of curves (g)–(i), where the decrease rates at the very beginning of the second deposition are almost the same,  $\Theta_{ad} \approx Rt$ , irrespective of  $\tau$ , while the decrease rate become slower after that from (f) to (i), because the deposition amounts at the first deposition stage are larger and  $\tau$  is smaller. Thus, the resistance change can be explained by the rate equation of  $\Theta_{ad}$ .

In the lower panel of Fig. 4, the resistance rises above the initial value in the interruption period after the first deposition, while Fig. 2 and the upper panel of Fig. 4 do not show such a phenomenon. This difference is considered to be caused by the different density of 2DAG on top of the initial  $\sqrt{3}$  surface. In the case of Fig. 2 and the upper panel of Fig. 4, we waited for one hour after the high-temperature preparation of the initial  $\sqrt{3}$  surface to cool the Si wafer down to RT, and then the conductance measurements with Ag deposition were started. But in the experiments of the lower panel in Fig. 4, the waiting time was only 30 min, so that the substrate temperature was considered to be a little higher. The higher substrate temperature enables more Ag adatoms to retain as 2DAG on top of the initial  $\sqrt{3}$  surface in thermal equilibrium, so that the initial resistance is lower. But once the sinks (stable 3D islands) are created on the surface by the first deposition, the equilibrium density of the 2DAG after the first deposition stops should be lower than the initial equilibrium density, resulting in a resistance larger than the initial value.

As mentioned so far, the decrease in resistance directly corresponds to the increase in the adatom density in 2DAG. But there are three points which are not clear at present.

The first is the moderate decrease in resistance after the overshoot [Figs. 2(a)–2(c)]. Since the nucleation of Ag is heterogeneous, preferential sites for nucleation will decrease during deposition, so additional nucleations have to begin at less preferential sites. This may cause the increase of critical supersaturation and also the increase of adatom density in 2DAG. Another explanation may be some effects of 3D nuclei on the electrical conductance.

The second point for open question is the shoulder in Figs. 2(c)–2(e) after the deposition stops. This may be explained as follows. The resistance first increases steeply due to the nucleation of new additional stable nuclei, and then its increase rate temporarily slows down because the supersaturation becomes small. Then, the resistance increases faster again because of a faster rate of capturing the adatoms in 2DAG due to a larger density of 3D nuclei. Thus the recovering rise in resistance can be divided into two processes: heterogeneous nucleation and growth of 3D microcrystals.

The third point, which is the most important, is the reason why the 2DAG makes the conductance extremely high. The surface electronic structure of the  $\sqrt{3}$  surface is found to be semiconductorlike,<sup>2,6</sup> and the surface Fermi level is always

located in the vicinity of the valence-band maximum,<sup>7</sup> so that its surface space-charge layer is a hole-accumulation layer, irrespective of the doping in the bulk. Johansson *et al.*<sup>8</sup> have found that electrons partly fill a dispersive surface-state band which originates from an antibonding state of Ag atoms. If additional electrons are donated into the surface-state band by adsorbing the Ag adatoms, the conduction through this surface-state band will be enhanced. The existence of the dilute Ag adatoms on top of the  $\sqrt{3}$  surface is already noticed in Refs. 7–9, and their effect on this surface-state band is also discussed in Ref. 8. Alternatively, the configuration of the surface-state band of the  $\sqrt{3}$  surface might be essentially

changed by additional Ag adsorption, so that the effects of new surface states or band bending in the surface space-charge layer might be brought about. Further studies by microscopies and spectroscopies are now in progress to confirm these guesses.

We acknowledge valuable discussions with Professor. S. Ino and Professor A. Natori. We also thank Professor M. Henzler for his critical reading of the manuscript. This work is supported by a Grant-In-Aid from the Ministry of Education, Science and Culture of Japan, and also by the Sumitomo Foundation.

---

<sup>1</sup>R. Kern, G. Le Lay, and J. J. Metois, in *Current Topics in Materials Science*, edited by E. Kaldis (North-Holland, Amsterdam, 1979), Vol. 3, Chap. 3.

<sup>2</sup>T. Takahashi and S. Nakatani, *Surf. Sci.* **282**, 17 (1993), and references therein; Y. G. Ding, C. T. Chan, and K. M. Ho, *Phys. Rev. Lett.* **67**, 1454 (1991); **69**, 2452 (1992); S. Watanabe, M. Aono, and M. Tsukada, *Phys. Rev. B* **44**, 8330 (1991).

<sup>3</sup>S. Hasegawa and S. Ino, *Phys. Rev. Lett.* **68**, 1192 (1992); *Surf. Sci.* **283**, 438 (1993); *Thin Solid Films* **228**, 113 (1993); *Int. J. Mod. Phys. B* **7**, 3817 (1993).

<sup>4</sup>A. Natori, M. Murayama, and H. Yasunaga, *Surf. Sci.* **357–358**, 47 (1996).

<sup>5</sup>M. Murayama, A. Natori, and H. Yasunaga, *Proc. Phys. Soc. J.* **2**, 539 (1996).

<sup>6</sup>T. Yokotsuka, S. Kono, S. Suzuki, and T. Sagawa, *Surf. Sci.* **127**, 35 (1983); J. M. Nicholls, F. Salvan, and B. Reihl, *Phys. Rev. B* **34**, 2945 (1986).

<sup>7</sup>S. Kono, K. Higashiyama, T. Kinoshita, H. Kato, H. Ohsawa, and Y. Enta, *Phys. Rev. Lett.* **58**, 1555 (1987).

<sup>8</sup>L. S. O. Johansson, E. Landemark, C. J. Karlsson, and R. I. G. Uhrberg, *Phys. Rev. Lett.* **63**, 2092 (1989); **69**, 2451 (1992).

<sup>9</sup>S. Kono, K. Higashiyama, and T. Sagawa, *Surf. Sci.* **165**, 21 (1986).